An improved dynamic Monte Carlo model coupled with Poisson equation to simulate the performance of organic photovoltaic devices

Lingyi Meng, Dong Wang, Qikai Li, Yuanping Yi, Jean-Luc Brédas, and Zhigang Shuai

Citation: The Journal of Chemical Physics **134**, 124102 (2011); doi: 10.1063/1.3569130
View online: https://doi.org/10.1063/1.3569130
View Table of Contents: http://aip.scitation.org/toc/jcp/134/12
Published by the American Institute of Physics

An improved dynamic Monte Carlo model coupled with Poisson equation to simulate the performance of organic photovoltaic devices

Lingyi Meng,[1] Dong Wang,[1] Qikai Li,[2] Yuanping Yi,[3] Jean-Luc Brédas,[3] and Zhigang Shuai[1,2,a)]

[1]*Key Laboratory of Organic OptoElectronics and Molecular Engineering, Department of Chemistry, Tsinghua University, 100084 Beijing, China*
[2]*Key Laboratory of Organic Solids, Beijing National Laboratory for Molecular Science (BNLMS), Institute of Chemistry, Chinese Academy of Sciences, 100190 Beijing, China*
[3]*School of Chemistry and Biochemistry and Center for Organic Photonics and Electronics, Georgia Institute of Technology, Atlanta, Georgia 30332-0400, USA*

(Received 1 November 2010; accepted 1 March 2011; published online 22 March 2011)

We describe a new dynamic Monte Carlo model to simulate the operation of a polymer-blend solar cell; this model provides major improvements with respect to the one we developed earlier [J. Phys. Chem. B **114**, 36 (2010)] by incorporating the Poisson equation and a charge thermoactivation mechanism. The advantage of the present approach is its capacity to deal with a nonuniform electrostatic potential that dynamically depends on the charge distribution. In this way, the unbalance in electron and hole mobilities and the space-charge induced potential distribution can be treated explicitly. Simulations reproduce well the experimental *I-V* curve in the dark and the open-circuit voltage under illumination of a polymer-blend solar cell. The dependence of the photovoltaic performance on the difference in electron and hole mobilities is discussed. © *2011 American Institute of Physics*. [doi:10.1063/1.3569130]

I. INTRODUCTION

Solar energy conversion is being recognized as an essential component of future global energy production given the need for renewable and clean energy resources.[1] In this context, organic polymer solar cells present potential benefits, such as low-cost and ease of fabrication, and incorporation into flexible and light-weight modules, which makes them interesting alternatives to conventional inorganic solar cells.[2]

Based on the concept of bulk heterojunction,[3] great improvements in the performance of polymer solar cells have been achieved in recent years with power conversion efficiencies (PCEs) now reaching 8%.[4] However, the PCEs of organic photovoltaic (OPV) devices, especially those of all-polymer solar cells,[5] are still lower than theoretical expectations,[6,7] which limits their commercialization opportunities. While the theoretical challenges that remain to be met in order to comprehensively understand the organic photovoltaic processes *at the molecular scale* have been discussed,[8] it is also highly desirable to try and develop accurate and reliable numerical descriptions of bulk heterojunction solar cells *at the device scale* in order to help in the optimization of their performance.

The photovoltaic processes in organic materials can be described by either the continuum equation method[9,10] [e.g., the Poisson equation (PE) coupled with a drift-diffusion equation] or a discrete model[11–14] [e.g., the dynamic Monte Carlo (DMC) model with the first reaction method (FRM)[15]]. The continuum equation method is able to reproduce the performance of solar cells and to describe quantitatively the key physical parameters playing a role in OPV devices, in particular the space charge effect. However, the impact of morphology is ignored, although it is well established that the PCE is very sensitive to the polymer nanostructure in addition to light absorption and charge mobility.[13]

In contrast to the continuum equation method, the DMC model can be used to investigate the morphological dependence of polymer blends.[13] In addition, the dynamical trajectories of the particles that appear in the device can be tracked and recorded for further investigations. These are important advantages in order to understand the dynamics of the photovoltaic processes. In earlier DMC simulations,[10,13] the electron and hole mobilities were assumed to be balanced, so that space charge accumulation effects could not be treated in such DMC models. However, it has been shown experimentally that the charge mobilities in two polymers forming an all-polymer solar cell can differ by at least 1 order of magnitude. For instance, in the polymer blend of poly(perylenediimide-*alt*-dithienothiophene)[5] (PPDI) and bis(thienylenevinylene)-substituted polythiophene[16] (PBTT) (which we investigated in a previous work[13]), the electron mobility is 1.3×10^{-2} $cm^2\ V^{-1}\ s^{-1}$ while the hole mobility is in the range of $10^{-4} \sim 10^{-3}$ $cm^2\ V^{-1}\ s^{-1}$. Importantly, the space charges accumulated in the device when there exists a large difference in electron and hole mobilities can limit the photocurrent significantly.[10,17] We note that, in our previous work, the *I-V* curve in the dark and the open-circuit voltage under illumination were not well described under the assumption of balanced electron and hole mobilities.[13]

To solve these issues, we have tried to improve the DMC model by coupling the FRM with the Poisson equation; this improved version is therefore referred to as the DMC-PE

a)Author to whom correspondence should be addressed. Electronic mail: zgshuai@tsinghua.edu.cn.

model. With an initial guess of the linearly distributed driving potential, the charge density distribution can be obtained after accumulation of the charges in the device and tracking of the dynamical trajectory for each particle in the DMC simulations; then, the space-charge induced potential distribution and the linear driving potential can be evaluated by solving the Poisson equation with the boundary condition for the electrostatic potential. The adjusted driving potential distribution further affects the charge density distribution by exerting an updated electric field on the charge carrier. This coupled process is repeated iteratively until the system eventually reaches a self-consistent state. It has been demonstrated that DMC coupled with the Poisson equation can reveal the space-charge accumulation effect in the photocurrent generation process.[18]

The performance of the solar cell in the dark represents a key intrinsic property of the device, with the dark current mainly originating from charge injection and thermal activation. Some conventional models such as Fowler–Nordheim tunneling[19,20] and Richardson–Schottky thermionic emission[20] have been utilized to analyze and investigate charge injection from the electrodes. However, a numerical simulation, e.g., via the DMC method, when based on reasonable assumptions, could provide a valuable and detailed description of the charge-injection process.[20]

II. MODEL AND COMPUTATIONAL APPROACH

As in our previous DMC implementation,[13] we consider a polymer blend of PPDI (Ref. 5) and PBTT (Ref. 16) and the parameters are chosen from the experimental data measured on this blend which is strongly absorbing. The system is discretized into a lattice of 60×60×30 sites in the x, y, and z directions, respectively. The lattice constant a_0 is set to 3 nm based on XRD data[21] and the system temperature T is 298 K. To evaluate the site energy of the charge carriers, Coulombic interactions with a cutoff distance R_c of 15 nm are calculated by taking into account the Gaussian standard deviation σ to the density of states; the dielectric constant ε of the polymer blend is fixed at 3.5.

The FRM is used to describe the complete process of photocurrent generation in the organic solar cell. The central concept of the FRM is a queue of events stored in the order of ascending waiting times τ_q. An event actually corresponds to a configurational change in the system and the queue of events is constantly updated to reflect the system evolution by executing the head event in the queue at every time. The waiting time τ_q is calculated as:

$$\tau_q = -\frac{1}{W}\ln(X), \tag{1}$$

where X is a random number uniformly distributed in the range (0, 1) and W is the rate of an event.

For excitons, the exciton generation rate $W_{eg} = 900\ s^{-1}\ nm^{-2}$ is calculated from the AM1.5 solar spectrum with an illumination of 90 mW/cm^2 and the absorption spectrum of the polymer blend.[5] At the donor/acceptor interface, exciton dissociation to charge carriers is a preferred event, so that the exciton dissociation rate W_{ed} must be set sufficiently high. The exciton hopping rate is calculated using a simplified Förster equation where the temperature dependence is removed,[13] because the site energy for excitons (being neutral particles) is set to zero. The parameters corresponding to exciton hopping include a prefactor $W_e R_0^6 = 2\ nm^6\ ps^{-1}$ in the Förster equation and an exciton recombination rate $W_{er} = 1/500\ ps^{-1}$, which are taken to ensure that the excitons have a diffusion length of about 10 nm.[2]

Once created, the charge carriers are assigned to three possible events, that is, hopping, charge recombination, or extraction by the electrodes. The hopping rate for the charge carriers is calculated using Marcus theory,[22]

$$W_{ij} = V_{hop}\exp\left(-\frac{(E_j - E_i + E_r)^2}{4E_r k_B T}\right), \tag{2}$$

where E_i and E_j are the energies of hopping sites i and j, respectively, and E_r is the reorganization energy corresponding to twice the polaronic binding energy.[12] The prefactor V_{hop} is derived from the Einstein relation under isoenergetic site condition:[11,12]

$$V_{hop} = \frac{6k_B T\mu_{e/h}}{qa_0^2}\exp\left(\frac{E_r}{4k_B T}\right), \tag{3}$$

where $\mu_{e/h}$ is the charge carrier mobility (assumed in our earlier work[13] to be equal for electrons and holes). When the electron and the hole are located on adjacent sites, they can recombine at a rate W_{cr}. A charge carrier adjacent to the electrode is extracted from the device with a rate W_{ce}, which is calculated by using the Marcus formula of Eq. (2); the energy difference (driving force) between the Fermi level of an Al electrode and the LUMO of PPDI is taken as $-E_{IB} = -0.4$ eV.

Based on this DMC model (all simulation details can be found in Ref. 13), the morphological dependence of the device was described, and strategies for the development of efficient polymer OPV devices were proposed. However, our earlier model was not able to reproduce the *I-V* curve in the dark, which is an important intrinsic property of the device.[5] In addition, the dependence of PCE on charge mobilities, especially on the difference in electron and hole mobilities, was not accounted for. Incorporation of the potential and charge density distributions is of great interest as soon as the electron and hole mobilities in the OPV device are not balanced. Thus, new mechanisms and related parameters were incorporated into the DMC-PE model.

The improvements achieved in the new DMC-PE model are as follows:

1. Charge injection

In our previous DMC implementation, both charge injection and charge extraction were governed by the same Marcus formula as that used for charge hopping. It has been suggested that charge injection is a key process that should be described by a more sophisticated method in order to simulate the dark current. The energy barrier U, which restricts the dark charge-carrier injection from a metallic electrode into the bulk of a polymer material, must be evaluated. The energy barrier was, in our earlier model, taken as E_{IB}, which corresponds to the energy difference between the LUMO of PPDI and the Fermi level of Al. More detailed investigations indicate that the

energy barrier U actually depends as well on the external electric field and the Coulomb field binding the carrier with its image twin in the electrode:[20,23,24]

$$U = E_{IB} - \frac{q^2}{16\pi\varepsilon_0\varepsilon a_0} - qFa_0, \tag{4}$$

where a_0 is the lattice constant, E_{IB} the barrier height in the absence of both electric field and image charge effect, F the electric field, q the elementary charge, ε the medium dielectric constant, and ε_0 the vacuum permittivity.

In the DMC-PE model, E_{IB} is set to 0.4 eV,[5] and the electric field F is obtained by solving the Poisson equation. The charge injection is restricted to the lattice sites in contact with an electrode, that is, the electron conductor lattice near the cathode and the hole conductor lattice near the anode; thus, the distance of the injection contact is fixed to the lattice constant in Eq. (4). The subsequent charge carrier motions in the device will take full account of the local electric field. Near the electrodes, the image charge effects are included up to a cutoff distance of 15 nm.

The conventional Miller–Abrahams expression[11,23] has been used to calculate the rate of a charge jumping from the Fermi level of the electrode to a site in the dielectric;[23] by considering the restriction on the injection sites, the Miller–Abrahams expression simplifies as:

$$W_{ij} = W_0 \begin{cases} \exp\left(-\dfrac{E_j - E_i}{k_B T}\right) & : E_i < E_j \\ 1 & : E_i \geq E_j \end{cases}, \tag{5}$$

where the prefactor W_0 is derived from the Einstein relation under isoenergetic site condition as:[13]

$$W_0 = \frac{6k_B T \mu_{e/h}}{qa_0^2}. \tag{6}$$

The Gaussian standard deviation σ to the density of states is taken into account in the calculation of the site energies for charge injection.[13] Therefore, the site energies are taken as $E_j = U + \sigma R$ and $E_i = \sigma R$, where R is a normally distributed random number and U is calculated by using Eq. (4).

We note that charge extraction near the electrodes remains described by the Marcus formula [Eq. (2)] as in our previous model. Only those charges adjacent to the electrodes can be extracted, with a limitation that the freshly generated charge carriers are not allowed to be extracted instantly. To be specific, any charge carrier created adjacent to the electrodes must hop at least one step in the polymer blend before it can be extracted.

These different treatments for charge injection and charge extraction can lead to appropriate charge densities adjacent to the electrodes, which enable us to numerically solve the Poisson equation.

2. Charge thermal activation

For a conventional inorganic solar cell, thermally activated charges represent another source of dark current in addition to charge injection. Therefore, exciton thermal activation is also incorporated into the FRM algorithm[13] to simulate the dark saturation current density J_{S} under reverse bias voltage. Thermally activated excitons undergo exciton diffusion and charge separation at the interface in the same way as photogenerated excitons. The generation rate for the thermally activated excitons is evaluated based on the dark saturation current density J_{S} under reverse bias voltage. In practice, the generation rate $W_{\mathrm{egt}} = 32\ \mathrm{s}^{-1}\ \mathrm{nm}^{-2}$ is set for thermally activated excitons, which leads to a dark current density $J_{\mathrm{S}} \approx 0.36\ \mathrm{mA/cm}^2$ under the external applied voltage of –1.5 V. This simulation result is consistent with the experimental dark saturation current density of $0.37\ \mathrm{mA/cm}^2$.[5]

3. Poisson equation

The coupled Poisson equation in the DMC-PE model is

$$\frac{\partial^2}{\partial z^2}\psi(z) = \frac{q}{\varepsilon_0\varepsilon}[n(z) - p(z)]. \tag{7}$$

This equation relates the potential $\psi(z)$ to the electron and hole densities $n(z)$ and $p(z)$ in the system. The Gummel iteration method[9] is utilized to solve the discretized Poisson equation. To simulate the device performance under dark condition for the polymer blend, the boundary condition for the potential in solving the Poisson equation can be set as

$$\psi(L_z) - \psi(0) = V_a, \tag{8}$$

where V_a is the external applied voltage and L_z is the device dimension in the z direction. This is based on the assumption that an organic photovoltaic device in the dark is in equilibrium in the case of zero external field ($V_a = 0$), which is similar to the situation in a traditional inorganic device.

Under illumination, the open-circuit voltage V_{OC} is limited by the light-induced splitting of the quasi-Fermi levels, which is related to the difference between the electron affinity (or crudely speaking the LUMO level) of the acceptor material and the ionization potential (HOMO level) of the donor material in the active layer. Therefore, the boundary condition for the potential in solving the Poisson equation under illumination is set as[9,10,25]

$$\psi(L_z) - \psi(0) = V_a - \frac{1}{q}E_{\mathrm{gap}}, \tag{9}$$

where E_{gap} is the energy difference between the electron affinity of the acceptor material and the ionization potential of the donor material.[5]

The solution to the Poisson equation with the boundary condition gives the total electrostatic potential due to space charge and a linearly distributed driving potential. It can be derived that the driving electric field is simply the average of the total electric field at the boundaries. In the DMC simulation, the charge drift is governed by the Coulombic interactions and the driving electric field obtained by solving the Poisson equation. The driving force due to the difference in the work functions between the electrodes is no longer considered. Thus all electrostatic or Coulombic interactions in the device have been included in the DMC-PE model.

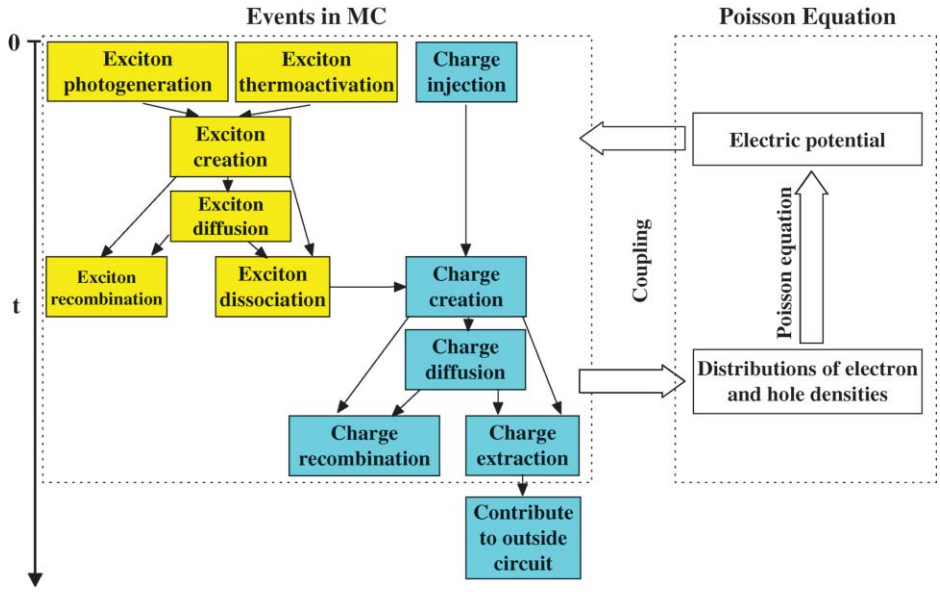

FIG. 1. Schematic representation of the simulation processes. The dynamic Monte Carlo method is extended by coupling to the Poisson equation.

4. Charge recombination

By considering charge injection and thermal activation, the charge accumulation process in the device is enhanced. The charge recombination rate is thus set at 10^{-5} ps^{-1} to balance the excess charge density. These values lead to a typical charge density of $\sim 10^{22}$ m^{-3} when the charge mobilities are set either to the same equal values as in the previous DMC simulations (e.g., $\mu_n = \mu_p = 10^{-3}$ cm^2 V^{-1} s^{-1}) (Ref. 13) or to different values as measured experimentally (e.g., $\mu_n = 10^{-2}$ cm^2 V^{-1} s^{-1} and $\mu_p = 10^{-4}$ cm^2 V^{-1} s^{-1}) for the polymer blend.[5]

All possible events in the DMC-PE model and the coupling between DMC and Poisson equation are sketched in Fig. 1, while all the parameters are listed in Table I. As the experimental morphology of the polymer blend is not known, we have used in the simulations an optimized blend morphology structure with a characteristic feature size of around 10 nm, which yields the peak PCE based on our previous investigation of the morphological dependence of the photovoltaic performance.[13] The detailed generation process and the parameters of the morphology have been provided in the Appendix.

III. RESULTS AND DISCUSSION

The simulated *I-V* curve in the dark for the polymer blend is shown in Fig. 2. It can be seen that our simulation results provide a consistent picture of the device performance under dark condition. Similar to the photogenerated current, the dark current is also sensitive to the morphology of the polymer blend. Note that an optimized morphology structure is used in the simulation, it is therefore not surprising to see that the ideal photo- and dark currents are both larger than the experimentally measured values. The experimental mobilities ($\mu_n = 10^{-2}$ cm^2 V^{-1} s^{-1}, $\mu_p = 10^{-4}$ cm^2 V^{-1} s^{-1}) are taken into account in the simulation.

For an ideal solar cell, it is assumed that the photogenerated current density J_{ph} is voltage independent, which means that J_{ph} is equal to the short-circuit current density J_{SC} at any applied voltage.[26,27] It follows that

$$J_L = J_D + J_{ph} \xrightarrow{J_{ph}=J_{SC}} J_D + J_{SC}, \tag{10}$$

where J_D and J_L are the dark current density and the current density under illumination, respectively. Thus, the *I-V* curve under illumination can be calculated based on the dark *I-V* curve by using Eq. (10), where J_{SC} is obtained from the direct DMC simulations at zero applied voltage. The simulated open-circuit voltage, which equals 0.64 V, is in excellent agreement with the experimental data (0.63 V),[5] as shown in Fig. 2. Near the open-circuit operating condition, the dark

TABLE I. Parameters used in the modeling.

T	298.0 K	Temperature
ε	3.5	Dielectric constant
a_0	3 nm	Lattice constant
R_c	15 nm	Cutoff distance
W_{eg}	900 s^{-1} nm^{-2}	Exciton creation rate for photogenerated excitons
W_{egt}	32 s^{-1} nm^{-2}	Exciton creation rate for thermoactivated excitons
$W_e R_0^6$	2 nm^6 ps^{-1}	Exciton hopping rate
W_{er}	2×10^{-3} ps^{-1}	Exciton recombination rate
E_r[a]	0.187 eV	Reorganization energy (equal to twice the polaron binding energy)
V_{hop} (p)	1.06×10^{-3} ps^{-1}	Charge hopping rate prefactor for holes
V_{hop} (n)	1.06×10^{-1} ps^{-1}	Charge hopping rate prefactor for electrons
σ[a]	0.062 eV	Gaussian standard deviation
W_{cr}	1×10^{-5} ps^{-1}	Charge recombination rate
E_{IB}	0.4 eV	Difference between LUMO (A) and Fermi level of aluminum cathode
E_{gap}	1.1 eV	Difference between LUMO (A) and HOMO (D)
J_S	0.36 mA/cm^2	Dark saturation current density

[a]The parameters marked with an asterisk are taken from Ref. 12.

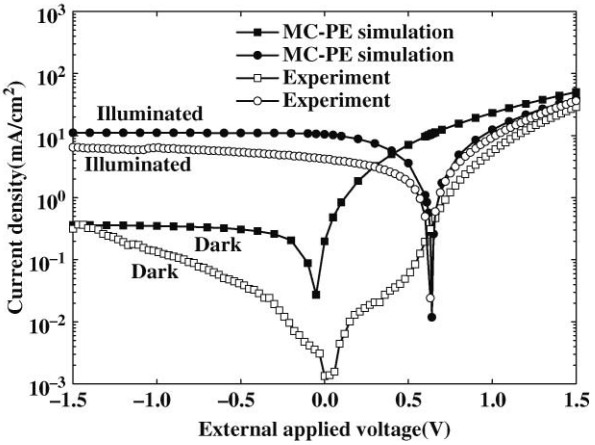

FIG. 2. Comparison of the *I-V* curves from the DMC-PE simulations and experiments. The illuminated current in the simulations is calculated by using Eq. (10).

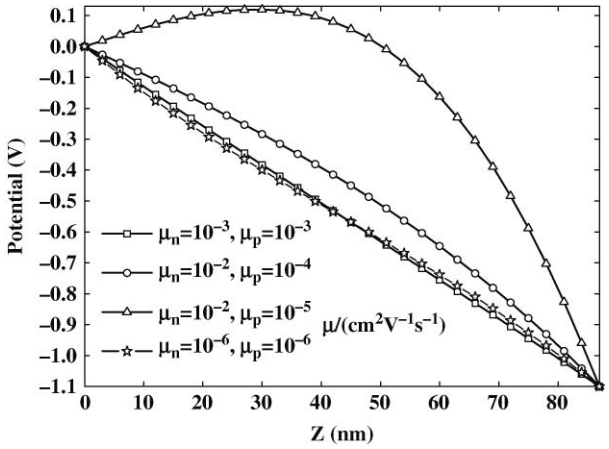

FIG. 3. The electrostatic potential distribution in the device under short-circuit condition. As the difference in hole and electron mobilities increases, the space charge accumulation effects are enhanced, which cause the potential to gradually deviate from the linear distribution.

current (in particular the injection dark current) has strongly increased and eventually cancels the photogenerated current. More precisely, near open-circuit operating conditions, two types of current are present, driven by different effective voltages that cancel each other. One is the injection current with the open-circuit voltage as the effective voltage, the other is the current coming from exciton dissociation for which the effective drive voltage is the open-circuit voltage shifted by the energy difference between the acceptor and donor materials E_{gap} [Eq. (9)].

These simulations provide convincing evidence that the DMC-PE model can improve our ability to describe the performance of organic solar cells, especially the dark *I-V* curve and the open-circuit voltage under illumination. The ability to simulate the performance of the device in the dark can expand our understanding of the photovoltaic device. As mentioned above, the appearance of the open-circuit voltage is due to the cancellation of the photogenerated current and the dark current. As a result, any approach that increases the photogenerated current relative to the injection current can enhance the open-circuit voltage. For example, it has been found that increasing the exciton dissociation rate,[28] which will surely increase the photogenerated current, is beneficial to the enhancement of the open-circuit voltage.

By incorporating the Poisson equation into the DMC model with FRM, the constraint of having to consider balanced mobilities for electrons and holes in the polymer blend is removed. Some of the key physical properties we are interested in, e.g., the potential and charge density distributions, can now be studied more appropriately.

As shown in Fig. 3, when electrons and holes have equal mobilities, the potential distribution in the OPV device is nearly linear; this confirms our previous assumption that, in a polymer blend with balanced carrier mobilities,[13,14] the charge drift is determined by a linear electric field. When mobilities for electrons and holes are different (here, $\mu_{\text{n}} > \mu_{\text{p}}$ for the polymer blend[5]), the potential distribution becomes more complicated and space charges begin to accumulate in the device. As a consequence, the electric field increases in the region near the anode to enhance the extraction of holes, as shown in Fig. 3, while in the region near the cathode the electric field decreases to suppress the extraction of electrons. As the difference in the mobilities of hole and electron increases, deviation from linearity for the potential distribution in the polymer blend is enhanced.

The corresponding charge densities in the polymer blend are shown in Fig. 4. The distributions are approximately

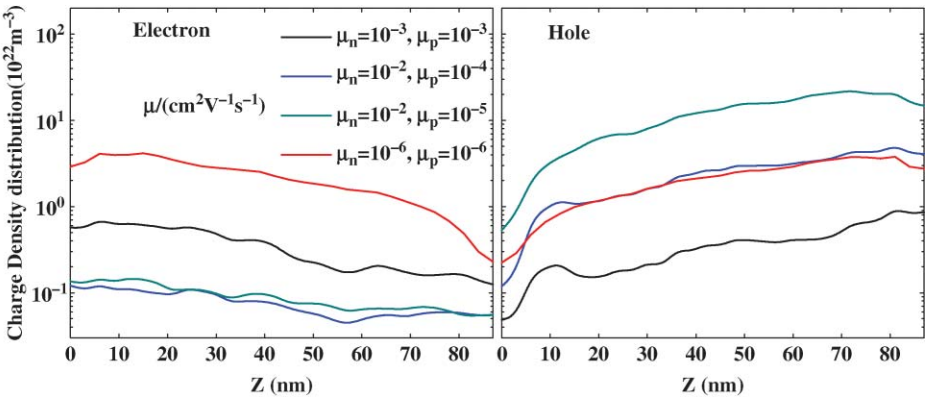

FIG. 4. Hole and electron density distributions in the device under short-circuit condition.

symmetric for electrons and holes in the polymer blend when the mobilities are balanced. However, the space charge accumulation controlled by the nonlinear potential distribution is gradually enhanced as the difference in mobilities of electron and hole increases.

With respect to the continuum equation method (or Poisson equation coupled with a drift-diffusion equation), the DMC-PE model used here actually provides for a discrete description of the particle hopping events in lieu of the drift-diffusion equation. The advantages of the continuum and discrete models have been combined to give a more appropriate description of the photovoltaic processes in organic solar cells.

IV. CONCLUSIONS

A DMC-PE model which combines the dynamic Monte Carlo method with the Poisson equation has been developed. In this model, the charge density distribution in a polymer blend is first evaluated; then, the updated potential solved by the Poisson equation is used to control the next round of charge motions in the polymer blend. This coupled model can be used to simulate the complex relationship between charge density and potential distributions in organic photovoltaic devices. The thermoactivation mechanism and a modified charge injection scheme have also been incorporated in the present model.

Based on the proposed DMC-PE model, the *I-V* curve in the dark and the open-circuit voltage have been simulated and found to be in good agreement with the experimental results. Such an agreement gives confidence that the microscopic mechanisms governing the operation of a polymer photovoltaic cell can be described reliably by the present approach. The DMC-PE model should prove to be a useful tool in the quest to design highly efficient photovoltaic cells, in particular in combination with better description of the molecular parameters.

ACKNOWLEDGMENTS

The authors are indebted to Professor A. B. Walker (University of Bath, UK) for helpful discussions. The work in Beijing was supported by the National Science Foundation of China (Grant for international collaboration No. 20920102031) and the work at Georgia Tech by the Office of Naval Research.

APPENDIX: MORPHOLOGY GENERATION

The Ising model is utilized to generate a series of blend morphologies with varying scales of phase separation. In the Ising model, up and down spins that occupy the node sites represent two constituting polymers (PPDI and PBTT) in the system. The number of up and down spins is identical in the system. The Hamiltonian for the energy contributed by site i is

$$\varepsilon_i = -\frac{J}{2}\sum_j (\delta_{s_i,s_j} - 1), \tag{A1}$$

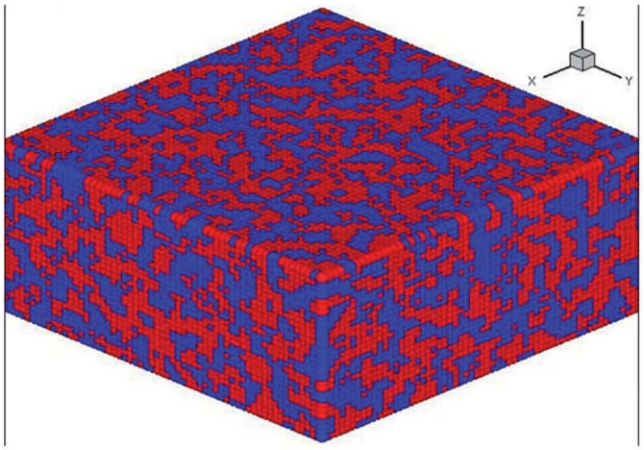

FIG. 5. The morphology used in the DMC-PE simulations.

where $\delta_{a,b}$ is the Kronecker delta function, and s_i, s_j are the spins occupying sites i and j. The summation over j includes all the first and second nearest neighbors, and the interaction energy is inversely proportional to the distance between sites i and j. For a cubic lattice, the scaling factor is $1/\sqrt{2}$ for the second nearest neighbors. An appropriate initial configuration and the interaction energy J are necessary to obtain a series of morphologies with different scales of phase interpenetration. The initial morphology with minimal phase separation is used in our simulations and the interaction energy J is set as $+k_BT$. To relax the system to an energetically favorable state, the Metropolis Monte Carlo simulation is performed. After a large number of trials and moves, a series of desired morphologies with varying scales of phase separation can be generated.

The dependence of the photovoltaic performance on the phase separation of the polymer blend has been previously investigated. An optimized blend structure which can lead to the peak PCE is chosen for the DMC-PE simulations presented in this work. The interfacial area of this blend structure (Fig. 5) is about 1.0×10^6 nm^2.

[1] J.-L. Brédas and J. R. Durrant, Acc. Chem. Res. **42**, 1689 (2009).
[2] S. Gunes, H. Neugebauer, and N. S. Sariciftci, Chem. Rev. **107**, 1324 (2007).
[3] G. Yu, J. Gao, J. C. Hummelen, F. Wudl, and A. J. Heeger, Science **270**, 1789 (1995).
[4] H. Y. Chen, J. H. Hou, S. Q. Zhang, Y. Y. Liang, G. W. Yang, Y. Yang, L. P. Yu, Y. Wu, and G. Li, Nat. Photonics **3**, 649 (2009).
[5] X. Zhan, Z. Tan, B. Domercq, Z. An, X. Zhang, S. Barlow, Y. Li, D. Zhu, B. Kippelen, and S. R. Marder, J. Am. Chem. Soc. **129**, 7246 (2007).
[6] M. C. Scharber, D. Mühlbacher, M. Koppe, P. Denk, C. Waldauf, A. J. Heeger, and C. J. Brabec, Adv. Mater. **18**, 789 (2006).
[7] G. Dennler, M. C. Scharber, T. Ameri, P. Denk, K. Forberich, C. Waldauf, and C. J. Brabec, Adv. Mater. **20**, 579 (2008).
[8] J.-L. Brédas, J. E. Norton, J. Cornil, and V. Coropceanu, Acc. Chem. Res. **42**, 1691 (2009).
[9] L. J. A. Koster, E. C. P. Smits, V. D. Mihailetchi, and P. W. M. Blom, Phys. Rev. B **72**, 085205 (2005).
[10] L. J. A. Koster, V. D. Mihailetchi, H. Xie, and P. W. M. Blom, Appl. Phys. Lett. **87**, 203502 (2005).
[11] P. K. Watkins, A. B. Walker, and G. L. B. Verschoor, Nano Lett. **5**, 1814 (2005).
[12] R. A. Marsh, C. Groves, and N. C. Greenham, J. Appl. Phys. **101**, 083509 (2007).

[13]L. Meng, Y. Shang, Q. Li, Y. Li, X. Zhan, Z. Shuai, R. G. E. Kimber, and A. B. Walker, J. Phys. Chem. B **114**, 36 (2010).
[14]M. Casalegno, G. Raos, and R. Po, J. Chem. Phys. **132**, 094705 (2010).
[15]J. J. Lukkien, J. P. L. Segers, P. A. J. Hilbers, R. J. Gelten, and A. P. J. Jansen, Phys. Rev. E **58**, 2598 (1998).
[16]J. Hou, Z. Tan, Y. Yan, Y. He, C. Yang, and Y. Li, J. Am. Chem. Soc. **128**, 4911 (2006).
[17]V. D. Mihailetchi, J. Wildeman, and P. W. M. Blom, Phys. Rev. Lett. **94**, 126602 (2005).
[18]F. Yang and S. R. Forrest, ACS Nano **2**, 1022 (2008).
[19]C. A. Spindt, I. Brodie, L. Humphrey, and E. R. Westerberg, J. Appl. Phys. **47**, 5248 (1976).
[20]S. Barth, U. Wolf, and H. Bässler, Phys. Rev. B **60**, 8791 (1999).
[21]J. Hou, C. Yang, C. He, and Y. Li, Chem. Commun. **8**, 871 (2006).
[22]R. A. Marcus, Rev. Mod. Phys. **65**, 599 (1993).
[23]U. Wolf, V. I. Arkhipov, and H. Bässler, Phys. Rev. B **59**, 7507 (1999).
[24]V. I. Arkhipov, U. Wolf, and H. Bässler, Phys. Rev. B **59**, 7514 (1999).
[25]M. Riede, T. Mueller, W. Tress, R. Schueppel, and K. Leo, Nanotechnology **19**, 424001 (2008).
[26]L. J. A. Koster, V. D. Mihailetchi, R. Ramaker, and P. W. M. Blom, Appl. Phys. Lett. **86**, 123509 (2005).
[27]S. M. Sze, *Physics of Semiconductor Devices* (Wiley, New York, 1981).
[28]Y. Shang, Q. Li, L. Meng, D. Wang, and Z. Shuai, Appl. Phys. Lett. **97**, 143511 (2010).